

Diet-Derived Phenolic Acids Regulate Osteoblast and Adipocyte Lineage Commitment and Differentiation in Young Mice

Jin-Ran Chen,^{1,2} Oxana P Lazarenko,^{1,3} Jian Zhang,^{1,2} Michael L Blackburn,^{1,3} Martin JJ Ronis,^{1,2,4} and Thomas M Badger^{1,2,3}

¹Arkansas Children's Nutrition Center, University of Arkansas for Medical Sciences, Little Rock, AR, USA

²Department of Pediatrics, University of Arkansas for Medical Sciences, Little Rock, AR, USA

³Departments of Physiology and Biophysics, University of Arkansas for Medical Sciences, Little Rock, AR, USA

⁴Departments of Pharmacology and Toxicology, University of Arkansas for Medical Sciences, Little Rock, AR, USA

ABSTRACT

A blueberry (BB)-supplemented diet has been previously shown to significantly stimulate bone formation in rapidly growing male and female rodents. Phenolic acids (PAs) are metabolites derived from polyphenols found in fruits and vegetables as a result of the actions of gut bacteria, and they were found in the serum of rats fed BB-containing diet. We conducted *in vitro* studies with PAs and demonstrated stimulation of osteoblast differentiation and proliferation. On the other hand, adipogenesis was inhibited. To more fully understand the mechanistic actions of PAs on bone formation, we administered hippuric acid, one of the major metabolites found in animal circulation after BB consumption, to prepubertal female mice for 2 weeks. We found that hippuric acid was able to stimulate bone-forming gene expression but suppress PPAR γ expression, leading to increased bone mass dose-dependently. Cellular signaling studies further suggested that the skeletal effects of PAs appeared to be mediated through activation of G-protein-coupled receptor 109A and downstream p38 MAP kinase and osterix. In conclusion, PAs are capable of altering the mesenchymal stem cell differentiation program and merit investigation as potential dietary therapeutic alternatives to drugs for degenerative bone disorders. © 2014 American Society for Bone and Mineral Research.

KEY WORDS: p38 MAP KINASE; BONE FORMATION; PPAR γ ; G-PROTEIN-COUPLED RECEPTOR

Introduction

Bone development is highly associated with genetics and gene-environment interactions.^(1,2) Bone mass accumulation during puberty (ages 12 to 18 years) results from substantial osteoblastic bone formation under the control of an array of genes that interact with endogenous hormones and environmental factors.⁽³⁾ Studies on the influences of diet on bone accretion in children have emphasized macronutrients (protein) and micronutrients (calcium and vitamin D). However, the human diet also contains a complex array of biologically active non-nutrient molecules, such as phytochemicals, that may act on and protect bone. These molecules interact with a wide range of endogenous genes that play significant roles in promoting skeletal development. Clinical data indicate that adequate intakes of phytochemical-rich fruit and vegetables in prepubescent children are an independent predictor of increased bone mass and size.^(4,5) To date, the most investigated effects of phytochemicals on bone are phytoestrogens (ie, isoflavones found in soy) and resveratrol (from red wine).⁽⁶⁾ The extent to

which these dietary factors can exert significant effects on bone formation and produce greater bone quality *in vivo* are still not fully verified.

Bone formation is dependent on the differentiation and activity of osteoblasts, whereas resorption of preexisting mineralized bone matrix by osteoclasts is necessary for bone remodeling.⁽⁷⁾ In rapidly growing animals, bone formation usually exceeds bone resorption, resulting in bone accrual. Bone marrow stromal cells and periosteal osteoblast precursors are both potential sources of new osteoblasts.⁽⁸⁾ Differentiation of mesenchymal stem cells toward tissue-specific lineages (for example, to either osteoblasts or adipocytes) is unexpectedly sensitive to environmental conditions.^(9,10) We have recently demonstrated a robust effect of blueberry (BB)-supplemented diets to stimulate bone formation in male and female rodents.⁽¹¹⁾ We have shown that BB diet has the ability to increase osteoblast numbers and osteoblast progenitor cell differentiation potential because of stimulation of p38 phosphorylation and downstream modulation of the activity of β -catenin and transcription factors such as Runx2.⁽¹¹⁾

Received in original form December 10, 2012; revised form June 4, 2013; accepted June 29, 2013. Accepted manuscript online July 6, 2013.

Address correspondence to: Jin-Ran Chen, PhD, Arkansas Children's Nutrition Center, Slot 512-20B, 15 Children's Way, Little Rock, AR 72202, USA.

E-mail: chenjinran@uams.edu

Additional Supporting Information may be found in the online version of this article.

For a Commentary on this article, please see Chen and Anderson (J Bone Miner Res. 2014;29: 1041–1042. DOI: 10.1002/jbmr.2234).

Journal of Bone and Mineral Research, Vol. 29, No. 5, May 2014, pp 1043–1053

DOI: 10.1002/jbmr.2034

© 2014 American Society for Bone and Mineral Research

This bone-promoting effect of BB diet may be produced by phenolic acids (PAs), which are gut microflora-derived metabolites of polyphenols found in the circulation after consumption of BB and other fruits, vegetables, and coffee.⁽¹¹⁾ PAs are structurally similar to nicotinic acid or niacin (the essential nutrient, vitamin B3), the nicotinic acid metabolite that binds and activates the G-protein-coupled receptor (GPR) 109A.⁽¹²⁾ We, therefore, hypothesized that the actions of PAs on bone cells may be mediated through mechanisms involving activation of GPR109A.

GPRs constitute the largest family of cell-surface molecules involved in signal transduction and cell differentiation, and have emerged as crucial players in child development, growth, and maturation.⁽¹³⁾ They are targets for many approved drugs. GPRs are capable of recruiting and regulating the activities of specific heterotrimeric G proteins, which are specialized signal transducers composed of three subunits: α , β , and γ . G proteins activate MAP kinase signaling, which is known to be important in many aspects of cell physiology including cell growth, survival, and differentiation.⁽¹⁴⁾ Several subtypes of GPRs have been shown to be involved in skeletal growth⁽¹⁵⁾ and obesity development;⁽¹⁶⁾ however, whether GPR109A plays a role in the pathway of osteoblast or adipocyte differentiation has not been previously examined.

In the present study, we present the *in vitro* and *in vivo* effects of the most abundant phenolic acid found in the serum of mice fed a BB-containing diet, hippuric acid (HA), on bone accrual in young mice. Herein we report that mice treated with HA have increased bone-forming gene expression and suppressed PPAR γ signaling, leading to increased bone mass in a dose-dependent manner. The skeletal effects appeared to be mediated through activation of G-protein-coupled receptor 109A and downstream p38 MAP kinase and osterix.

Materials and Methods

Animals and HA treatment

Female C57BL/6J mice were purchased from the Jackson Laboratory (Bar Harbor, ME, USA). Subsequently, these postnatal day (PND) 25 mice were randomly assigned to one of five groups ($n = 5$). All five groups of mice received AIN-93G diet formulated with casein as the sole protein source throughout the experiment. One group received a daily injection of saline peritoneal and was designated as the control group (control). The other four groups of mice received HA 0.1, 0.5, 1, or 5 mg/kg/day, designated as 0.1, 0.5, 1, and 5 HA groups, respectively. These doses were based on serum HA concentrations of mice fed a BB-containing diet and *in vivo* ferulic acid experiments in mice.⁽¹⁷⁾ All five groups were pair-fed, and the food and caloric intakes among all five groups were tightly controlled. Mice were housed in an Association for Assessment and Accreditation of Laboratory Animal Care-approved animal facility at the Arkansas Children's Hospital Research Institute with constant humidity and lights on from 6:00 a.m. to 6:00 p.m. at 22°C. All animal procedures were approved by the Institutional Animal Care and Use Committee at University of Arkansas for Medical Sciences (UAMS, Little Rock, AR, USA). After 14 days of injections (age PND40), mice were anesthetized by injection with 100 mg Nembutal/kg body weight (Lundbeck Inc., Deerfield, IL, USA), followed by decapitation, and leg bones and serum were collected.

Bone analyses

For the bone analysis, peripheral quantitative computerized tomography (pQCT) was first performed on formalin-fixed right tibia for bone mineral density measurement using a method well established in our laboratory⁽¹⁸⁾ using a STRATEC XCT 960 M unit (XCT Research SA, Norland Medical Systems, Fort Atkins, WI, USA) specifically configured for small bone specimens. Software version 5.4 was used with thresholds of 570 mg/cm³ to distinguish cortical bone and 214 mg/cm³ to distinguish trabecular from cortical and subcortical bone. Tibial bone mineral density (BMD) and bone mineral content (BMC) were automatically calculated. The position for pQCT scanning was defined at a distance from proximal tibia growth plate corresponding to 7% of the total length of the tibia. Distance between each scanning was 1 mm, and a total of five scans (five slices) were carried out. Data were expressed as the mean of three contiguous slices with the greatest trabecular bone density.

After pQCT scan, micro-computed tomography (μ CT) measurements of the trabecular from the right tibial bone were evaluated using a Scanco μ CT scanner (μ CT-40; Scanco Medical AG, Bassersdorf, Switzerland) at 6 μ m isotropic voxel size with X-ray source power of 55 kV and 145 μ A and integration time of 300 ms. The grayscale images were processed by using a low-pass Gaussian filter ($\sigma = 0.8$, support = 1) to remove noise, and a fixed threshold of 220 was used to extract the mineralized bone from the soft tissue and marrow phase. Cancellous bone was separated from the cortical regions by semi-automatically drawn contours. A total of 120 slices starting from about 0.1 mm distal to growth plate, constituting 0.70 mm length, was evaluated for trabecular bone structure based on description by Bouxsein and colleagues⁽¹⁹⁾ and by using software provided by Scanco, as described in detail previously.⁽²⁰⁾

At euthanization, calcein-labeled, left rear tibial bones were removed and fixed; sequential dehydration was carried out using different concentrations of alcohol. For the calcein labeling of bone *in vivo*, we sequentially injected calcein 20 mg/kg of body weight 1 week before death for the first time and 3 days before death for the second time. Proximal tibial bone samples were embedded, cut, and Masson stained by Histology Special Procedures. For histomorphometric analysis, sections were read in a blinded fashion. Parameters of cancellous bones in the proximal tibia and tibial shaft were measured with a digitizing morphometry system, which consists of an epifluorescent microscope (model BH-2, Olympus, Imaging America Inc. Center Valley, PA, USA), a color video camera, and a digitizing pad (Numonics 2206, Numonics, Montomerville, PA, USA) coupled to a computer (Sony Corporation of America, New York, NY, USA) and a morphometry program OsteoMetrics (OsteoMetrics, Inc., Decatur, GA, USA). Total bone area, osteoid surface, osteoblast number and surface, osteoclast number and surface, eroded surface, osteoid area, and single- and double-labeled perimeters were obtained by manual tracing as described by Dempster and colleagues.⁽²¹⁾

Serum bone formation marker

The serum bone formation marker, bone-specific alkaline phosphatase (ALP), was measured by Rat-MID ALP ELISA, from Nordic Biosciences Diagnostic (Herlev, Denmark).

Cell culture

Bone marrow stromal cell line ST2, bi-potential C2C12 cells, pre-adipocyte cell line 3T3-L1, and osteoblastic cell line OB6 were

cultured in α -MEM supplemented with 10% fetal bovine serum (FBS) (Hyclone, Logan, UT, USA), penicillin (100 Units/mL), streptomycin (100 μ g/mL), and glutamine (4 mM). These cell cultures were previously described in our laboratory.^(11,22) Mouse bone marrow cells were isolated from control diet animals and cultured in α -MEM according to a method published previously.⁽²²⁾ For different assay purposes (mRNA, cell staining, proteins), different sizes of cell culture plates were used and cells were treated in the presence or absence of individual PAs or a PA mixture, for different durations (see Results). Pretreatment of ST2 cells with PA was performed before rosiglitazone (Sigma, St. Louis, MO, USA) was added. Standard ALP activity, von Kossa and Oil Red O staining were performed in cell culture according to methods published previously.^(23,24) Transfection of GPR109A shRNA (Thermo Scientific, Waltham, MA, USA; catalog number RMM3981-9570161) or GPR109A overexpression plasmid (Ori-Gen Technologies, Framingham, MA, USA; catalog number MC211930) into ST2 cell was performed using protocols provided by the manufacturer. Empty vectors of pLKO.1 and pCMV6 Entry were used as control for GPR109A shRNA and overexpression plasmid, respectively. Nonradioactive cell proliferation assay was performed following protocol provided by the manufacturer (Promega, San Luis Obispo, CA, USA; Part#TB169).

Western blotting and co-immunoprecipitation

Right tibial bone tissue, after aspiration of bone marrow cells, and in vitro cellular proteins were extracted for western immunoblot analysis using cell lysis buffer as described previously.⁽²³⁾ Western blot and co-immunoprecipitation analyses were performed using standard protocols. The following primary antibodies were used: GPR109A, rabbit, polyclonal (Santa Cruz Biotechnology, Santa Cruz, CA, USA; cat. #sc-134583); phospho-p38, mouse monoclonal (Santa Cruz Biotechnology, cat. #sc-7973); p38, rabbit, polyclonal (Cell Signaling, Danvers, MA, USA; cat. #9212); myosin II, rabbit, polyclonal (Biomedical Technologies Inc., Stoughton, MA, USA; cat. #BT-567); osterix, rabbit, polyclonal (Bioss Inc.; cat. #bs-1110R); beta-actin, mouse, monoclonal; PPAR γ , rabbit, polyclonal (Abcam, Cambridge, MA, USA; cat. #ab19481). Secondary antibodies were purchased from Santa Cruz Biotechnology. Blots were developed using chemiluminescence (Pierce Biotechnology, Rockford, IL, USA) according to the manufacturer's recommendations.

RNA isolation, real-time reverse transcription-polymerase chain reaction

Cell RNA isolation from in vivo tissues or cultured cells were extracted using TRI Reagent (MRC Inc., Cincinnati, OH, USA) according to the manufacturer's recommendation, followed by DNase digestion and column cleanup using Qiagen (Valencia, CA, USA) mini columns.⁽²³⁾ Reverse transcription was carried out using an iScript cDNA synthesis kit from Bio-Rad (Hercules, CA, USA). All primers for real-time PCR analysis used in this study were designed using Primer Express software 2.0.0 (Applied Biosystems, Carlsbad, CA, USA).

Statistical analyses

Numerical variables were expressed as means \pm SEM (standard error of mean). Comparisons between groups were performed with the nonparametric Kruskal-Wallis test, followed by two-by-two comparisons performed with Mann-Whitney *U* test adjusted for multiple comparisons. For paired measures, the nonparamet-

ric Wilcoxon matched-pairs signed-ranks test was used. The critical *p* value for statistical significance was *p* = 0.05.

Results

Phenolic acids stimulate osteoblast differentiation and proliferation

We have characterized the in vitro bone-promoting properties of seven PAs found in rat serum after consumption of a BB-containing diet.⁽¹¹⁾ Molecular structures of these PAs are presented (Fig. 1A).⁽¹¹⁾ Our intent was to determine if a PA mixture (composed of seven PAs; Fig. 1A) or an individual PA, at the range of concentrations found in serum of rats fed a BB diet, can stimulate osteoblastic cell differentiation and proliferation. Bone marrow ST2 stromal cell line was treated with the PA mixture or seven individual PAs at five different concentrations based upon previous studies in rats.⁽¹¹⁾ The serum concentrations of each PA after feeding a BB diet containing 10% of calories as BB were used to determine the doses used in in vitro cell cultures.⁽¹¹⁾ The concentrations ranged from 0.1 \times to 2 \times the levels found in rat serum, where 1 \times represented the level found in serum of rats fed BB at 10% of calories. ALP mRNA expression, a well-known osteoblast differentiation marker, was dose-dependently upregulated by HA, 3-(3-hydroxyphenyl) propionic acid (PPA), and the PA mixture, whereas the other five PAs had minor or no effects on ALP mRNA expression (Fig. 1B). HA was further tested for its ability to induce osteoblast differentiation in cultures of the pluripotent ST2 cells, bipotent preosteoblastic C2C12 cells, and primary mouse bone marrow stromal cells (Fig. 1C). With the exception of 1 \times PA mixture in OB6 cells, cell proliferation assay revealed that HA and PA mixture at 0.5 \times and 1 \times significantly stimulated mature osteoblastic cells (OB6 cells), preosteoblastic cells (C2C12), and ST2 cell proliferation (Fig. 1D). These stimulatory effects of either HA or a PA mixture on cell proliferation tended to be dose-dependent in C2C12 and C2C12 cells.

In sharp contrast, HA and the PA mixture dose-dependently inhibited 3T3-L1 cell proliferation (Fig. 1D, E). 3T3-L1 cells are committed pre-adipocytes.⁽²⁵⁾ Therefore, they are widely used for studying adipogenesis and the biochemistry of adipocytes. Rosiglitazone is a peroxisome proliferator-activated receptor γ (PPAR γ) agonist; it is able to stimulate adipose differentiation in a dose-dependent manner with a maximum effect at a concentration of 2 to 5 μ M.⁽²⁶⁾ Treatment of ST2 cells with HA dose-dependently suppressed both endogenous PPAR γ and a biomarker of mature adipocytes, adipocyte fatty acid-binding protein 4/adipocyte Protein 2 (Fabp4/aP2) gene expression (Fig. 2A). We, therefore, next tested whether HA is able to inhibit rosiglitazone-induced adipogenesis. Compared with vehicle-treated control ST2 cells, both 0.5 μ M and 5 μ M rosiglitazone stimulated fat accumulation in a dose-dependent manner as shown by Oil Red-O staining (Fig. 2B). When cells were pretreated with HA, rosiglitazone-induced adipogenesis was blocked by HA in a dose-dependent manner (Fig. 2B). Surprisingly, when the mouse embryonic fibroblast cell line 3T3-L1 pre-adipocytes were treated with HA for 12 days, these cells took on phenotypical attributes similar to osteoblasts, showing positive ALP staining indicating formation of osteoblast-like cells (Fig. 2C). These osteoblastic-like cells were not only positively stained for ALP but also expression of multiple osteogenic markers was significantly increased, including osteocalcin (OC), osteopontin (OPN), and collagen type-I (COLI) (Fig. 2D). On the other hand, expression of

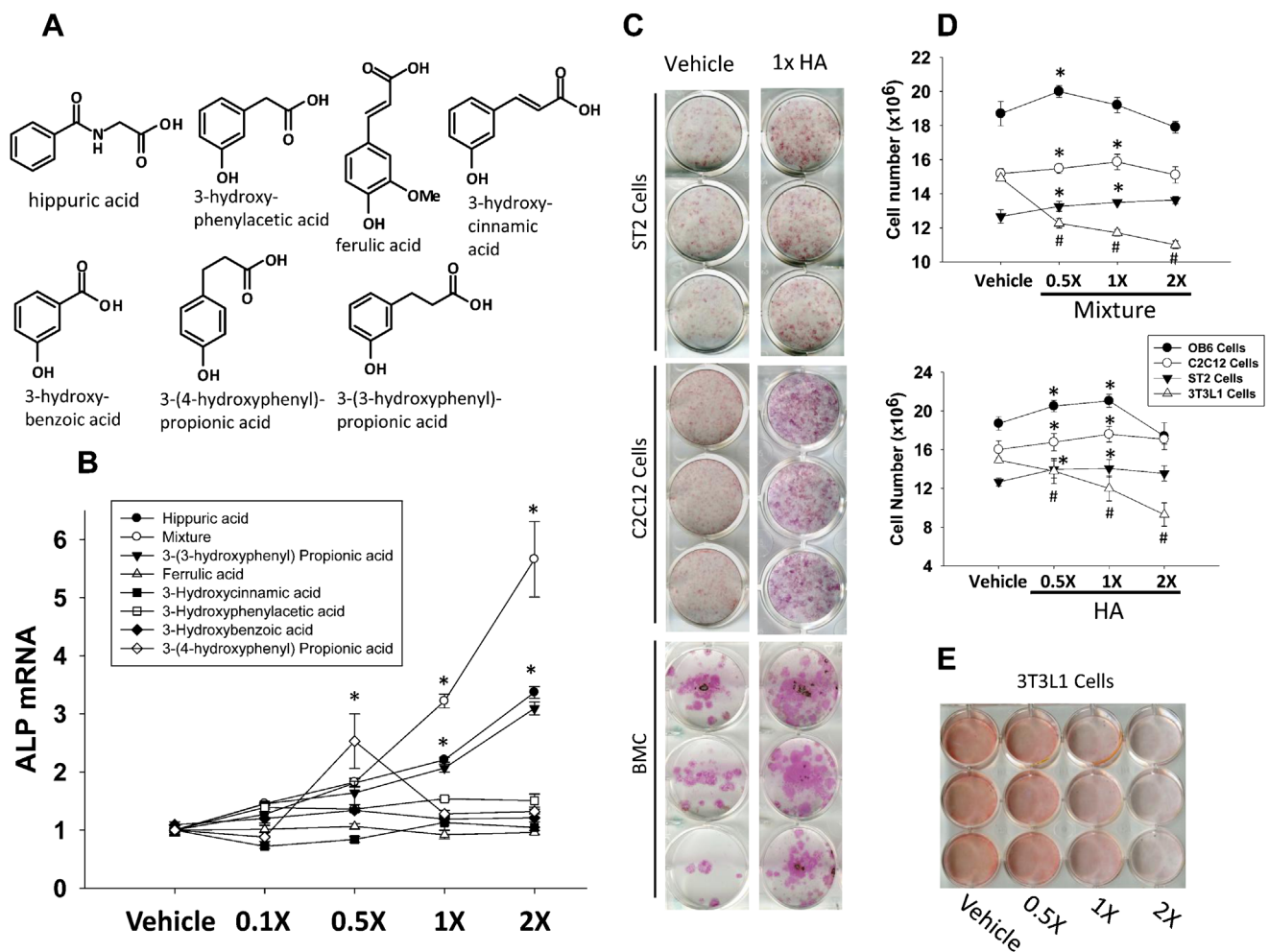


Fig. 1. PAs stimulate in vitro osteoblastic cell differentiation and proliferation. (A) Structures of seven PAs we identified in serum of BB-fed rats. (B) Of these PAs, HA and propionic acid dose-dependently stimulated the osteoblast differentiation marker ALP gene expression in ST2 cells. The concentrations found in serum of control casein and BB diet animals were 0.1 \times and 1 \times , respectively. (C) HA stimulated osteoblast mineralization (ALP staining) in ST2, C2C12, and primary mouse bone marrow cells after 12 days of treatment. (D) PAs increased osteoblastic cell numbers (OB6, ST2, and C2C12 cells) but inhibited preadipocyte (3T3L1 cells) proliferation after 3 days of treatment. (E) Oil Red-O staining of 3T3L1 cells after 3 days of treatment with different doses of HA (triplicates). Data are expressed as mean \pm SEM from triplicates of cell treatments ($n = 3$ /group). Significant differences are indicated by $p < 0.05$, *, #, compared with either 1 \times or vehicle treatment.

adipogenic markers, including aP2 and PPAR γ , were significantly decreased in these cells after HA treatment (Fig. 2D). These results suggest that HA is not only able to stimulate osteoblast differentiation but also is able to inhibit adipogenesis.

HA stimulates bone formation in rapidly growing mice

PA's effects on stimulating osteoblast differentiation in vitro led us to test the effect of HA on bone in vivo. Weanling female mice were injected ip with four doses of HA (0.1 to 5.0 mg/kg/day) daily for 14 days. Micro-CT scan revealed that HA significantly increased trabecular bone acquisition (Fig. 3A). Although 6-week-old mice are still in the rapidly growing phase, trabecular bone accumulation is close to maximal levels by this time. Treatment of mice with 1 and 5 mg/kg/day HA significantly increased trabecular bone; trabecular bone volume (BV/TV) was increased by about 10% and 20%, respectively, compared with those in control animals (Fig. 3A). These increases in bone acquisition were characterized by significant elevated trabecular numbers

(Tb.N, Fig. 3A) and significant decreases in trabecular spacing (Tb.Sp, Fig. 3A). Interestingly, trabecular thickness (Tb.Th, Fig. 3A) did not show differences. Serum ALP levels, a bone formation marker, was increased significantly in all HA-treated groups compared with control (Fig. 3B). The differences in bone phenotypes between control and HA-treated animals were confirmed by measurement using peripheral quantitative CT scan (pQCT), where tibial bone was scanned 1 mm below the growth plate (Supplemental Table S1). Trabecular bone mineral densities were significantly higher in 1 and 5 mg/kg/day HA-treated animals compared with their controls (Supplemental Table S1). Furthermore, static and dynamic histomorphometric analyses showed that osteoblast number and mineralizing surface per bone surface (Ms/Bs) were significantly increased in 1 and 5 mg/kg/day HA-treated animals compared with untreated controls (Fig. 3C). Bone formation rate was significantly increased in 0.5, 1, and 5 mg/kg/day HA-treated animals compared with untreated controls (Fig. 3C). Interestingly, osteoclast number was

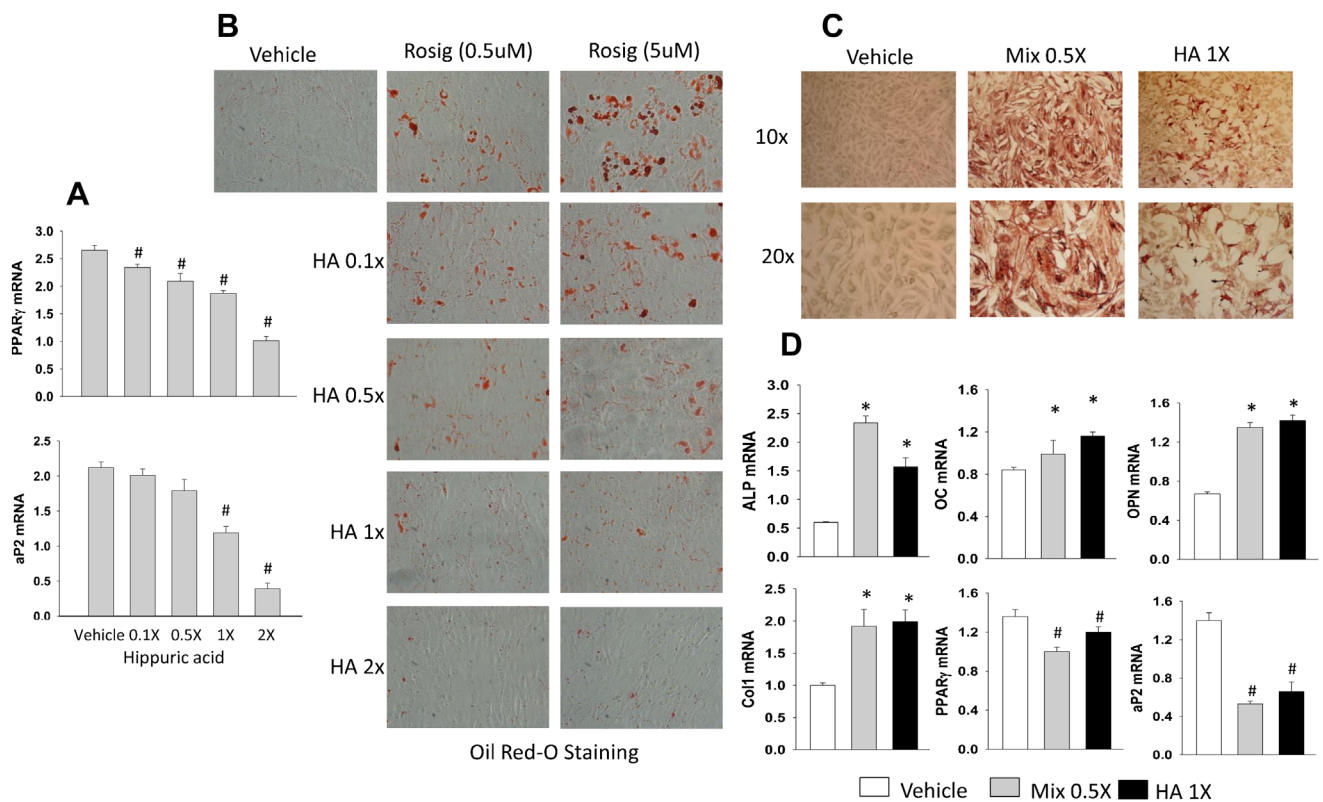


Fig. 2. PAs inhibit in vitro adipogenesis. (A) HA dose-dependently suppressed endogenous PPAR γ and aP2 gene expression in ST2 cells. (B) ST2 cells were pretreated with different concentrations of HA for 2 hours, and then continuously with rosiglitazone for an additional 5 days. Oil Red-O staining showed HA dose-dependently inhibited rosiglitazone-induced adipogenesis. (C) Pre-adipocyte 3T3L1 cells were treated with vehicle, 0.5 \times PA mixture (Mix 0.5 \times) or 1 \times HA (HA 1 \times) for 12 days. ALP staining showed colonies positive only in Mix 0.5 \times - and HA-1 \times -treated wells (presented both 10 \times and 20 \times magnification pictures). (D) RNA were isolated from pre-adipocyte 3T3L1 cells treated with vehicle, Mix 0.5 \times , or HA 1 \times for 12 days, and real-time PCR showed gene expression changes on markers for osteoblast and adipocyte differentiations. Similar results were obtained from three replicated experiments. Data are expressed as mean \pm SEM from triplicates of cell treatments. Significant differences indicated by $p < 0.05$, *, # compared with vehicle treatment.

significantly lower in all HA-treated animals compared with untreated controls (Fig. 3C). After aspiration of bone marrow, femur bone protein and RNA were isolated for western blot and real-time PCR analysis of signaling transduction. These analyses showed that GPR109A, phos-p38, myosin, and osterix protein expression were increased in HA-treated animals compared with their respective controls (Fig. 4A). Nonmuscular myosin has been suggested to be involved in osteoblast differentiation.⁽²⁷⁾ On the other hand, PPAR γ expression was downregulated in HA-treated animals compared with control (Fig. 4A). In accordance with these data, mRNA expression patterns of bone ALP, GPR109A, and osterix were also increased in HA-treated animals (Fig. 4B). Similarly, PPAR γ mRNA expression decreased dose-dependently in bone from HA-treated animals (Fig. 4B).

GPR109A is a mediator for HA to stimulate bone formation

We have shown that HA activated GPR109A, p38, and osterix, an essential transcription factor for osteoblast differentiation in bone. Whether these factors truly interact with each other in bone or osteoblasts to increase osteogenic signaling was therefore investigated. Immunoprecipitation was carried out using proteins isolated from bone and osteoblastic cells. Equal amounts of proteins were precipitated by GPR109A antibody.

Immunoblots showed increased protein levels of GPR109A, p-p38, and osterix, and their associations were significantly increased in 0.5, 1, and 5 mg/kg/day HA-treated animal groups compared with control (Fig. 5A). Similarly, when the same amounts of proteins were precipitated by phospho-p38, immunoblots showed an increase in protein levels of p-p38, GPR109A, and osterix in HA-treated (0.5, 1, and 5 mg/kg/day) groups compared with control (Fig. 5B). These in vivo results were recapitulated in mesenchymal stromal ST2 cells or mature osteoblastic OB6 cells treated with 1 \times HA for 24 hours (Fig. 5C, D).

GPR109A is expressed in a variety of cells and tissues, with the highest expression being in OB6 cells and bone marrow among the cells and tissues we have checked (Fig. 6A). In ST2 cells, PAs increased GPR109A mRNA expression, especially HA, which increased GPR109A expression in a dose-dependent manner (Fig. 6B). When GPR109A was knocked down using shRNA (Fig. 6C mRNA level; Fig. 6D protein level) in ST2 cells, nonmuscular myosin 2 expression was downregulated (Fig. 6D). In accordance with this finding, the expression of osteoblastic cell differentiation markers ALP and Runx2 were decreased in cells after shRNA (Fig. 6E). On the other hand, endogenous PPAR γ expression was increased in ST2 cells after shRNA GPR109A treatment (Fig. 6E). Most importantly, PAs were ineffective in stimulation of

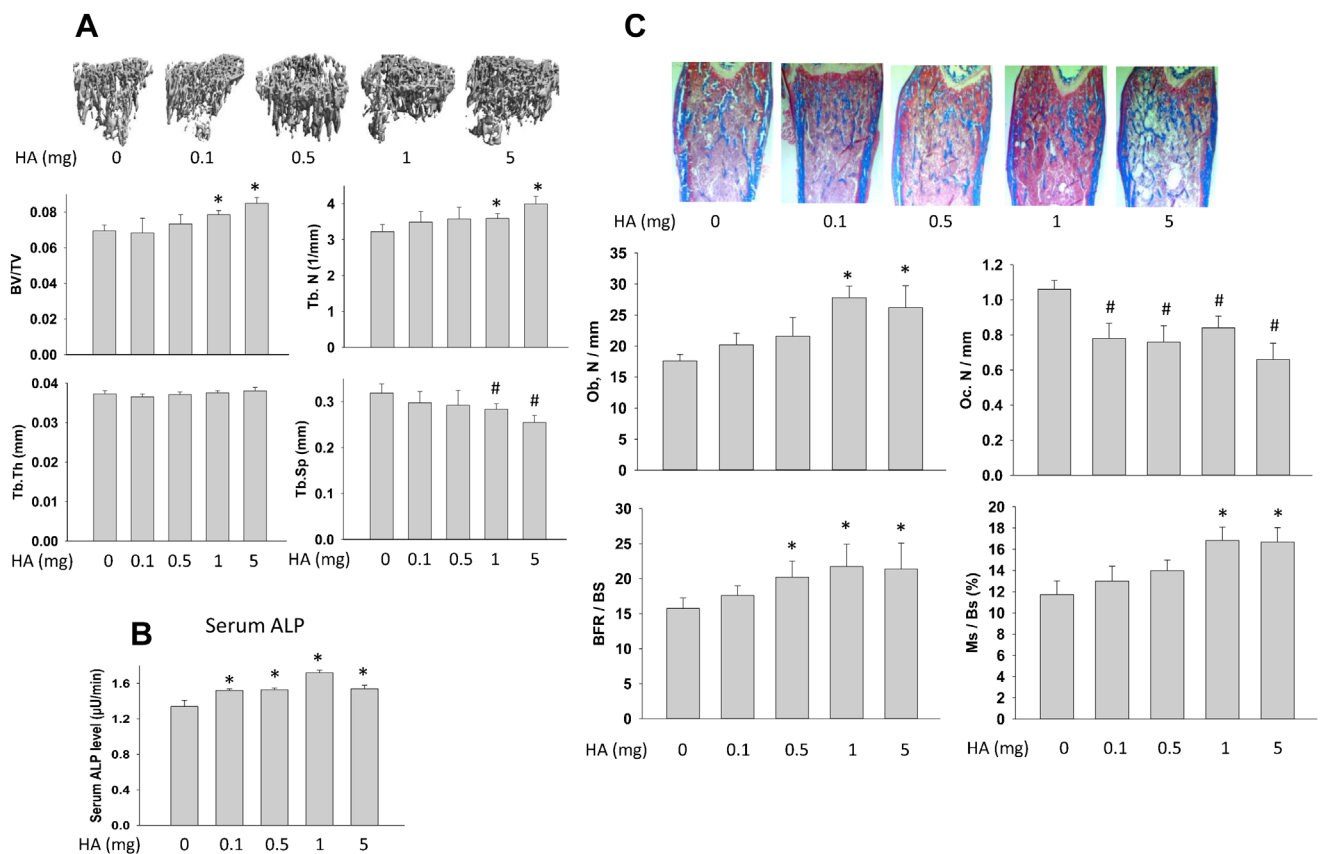


Fig. 3. HA stimulates in vivo bone formation in young mice. (A) Top panels are representative images from micro-CT analysis of the proximal tibia in mice treated with four HA doses in vivo. Bar graphs show quantitative micro-CT analysis of the proximal tibia in five different treatments of mice ($n = 5/\text{group}$). BV/TV (%) = bone volume/tissue volume; Tb.N (no./mm) = trabecular number; Tb.Th (mm) = trabecular thickness; Tb.Sp (mm) = trabecular spacing. (B) ELISA shows increased ALP activity in serum of HA-treated mice. (C) Static and dynamic histomorphometric parameters from five different diets of mice. Pictures are representatives of histomorphometric Masson staining from different diet mouse proximal tibia and blue color indicates bone. Numbers and bar graphs are from histomorphometric reading. Ob.N = osteoblast number; Oc.N = osteoclast number; BFR/BS = bone formation rate per bone surface ($\mu\text{m}^3/\mu\text{m}^2/\text{year}$); Ms/Bs = mineralizing surface per bone surface (%). Data bars are expressed as mean \pm SEM ($n = 5/\text{group}$). Significant differences indicated by $p < 0.05$, *, # compared with control animals.

osteoblastic cell differentiation after GPR109A was knocked down; this was estimated by ALP expression in ST2 cells (Fig. 6F) and mineralization analysis using von Kossa staining after 25 days of cultures (Fig. 6H). Conversely, overexpression of GPR109A in ST2 cells (stable transfection of GPR109A plasmid) increased phosphorylation of p38 and osterix expression but suppressed PPAR γ protein expression (Fig. 6G). Taken together, these data indicated that PAs stimulate osteoblast differentiation through activation of GPR109A.

Discussion

Recent studies have shown that bone formation is greater in rats fed diets containing BB, and in vitro data suggest that the PA class of polyphenol metabolites may be the bioactive components of BB responsible for these effects.^(11,28) Herein, we have presented results further suggesting that increased PAs in the circulation of rodents may be one of the causative factors responsible for bone formation associated with feeding BB diets. Among circulated PAs, HA and propionic acid were found at the highest concentration in serum after BB feeding⁽¹¹⁾ and were

found to be bioactive and able to stimulate osteoblast differentiation and bone formation both in vitro⁽¹¹⁾ and in vivo (present study). Although other PAs (for example, propionic acid) may have different potencies than HA to stimulate osteoblast differentiation, our data suggest that they exert effects through mechanisms similar to HA. The actions of PAs may represent a novel mechanistic paradigm by which BB-rich diets stimulate bone formation. PAs appear to activate osteoblast differentiation signaling pathways through initiation and activation of cell membrane GPR109A, which is known to bind nicotinic acid in many other cell types.⁽²⁹⁾

Our data also suggest that PAs inhibit adipogenesis and may even reverse this process in bone marrow. We speculate that adipocyte-precursors revert to cells with multidifferentiation potential and which can then further transdifferentiate toward the phenotype of osteoblastic cells (Fig. 2). Thus, these data provide circumstantial evidence to suggest that treatment of lineage-restricted somatic cells with exogenous factors such as PAs may be capable of reprogramming or transforming the cells from a committed to an uncommitted state. Thus, our findings lead us to propose a novel idea that dietary factors such as PAs

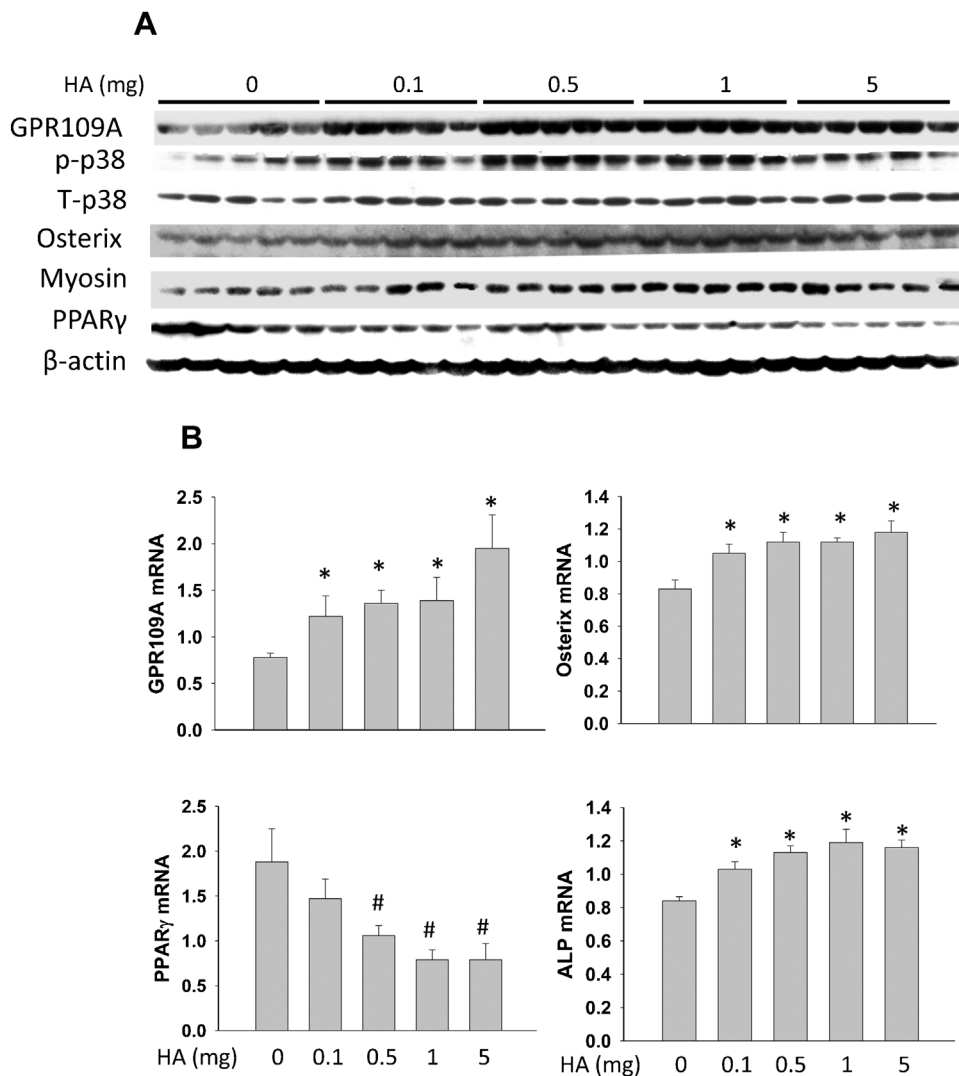


Fig. 4. HA activates GPR109A, p38, and osterix in bone. (A) Western blots indicate increased GPR109A, p38, myosin, and osterix activation but suppression of PPAR γ in bone from HA-treated mice. (B) Real-time PCR shows increased ALP, GPR109A, and osterix mRNA but dose-dependent decreased expression of PPAR γ in bone from HA-treated animals. Data bars are expressed as mean \pm SEM ($n = 5$ /group). Significant differences indicated by $p < 0.05$, *, # compared with control animals.

derived from polyphenols in BB diets are capable of altering stem cell differentiation programming and merit more detailed investigation as therapeutic alternatives to drugs for degenerative bone disorders.

PAs described in the current study are a group of small molecules found in the peripheral circulation after GI digestion of polyphenols. Among phytochemicals, polyphenols have been an emphasis of studies because of their suggested protective effects on several chronic diseases/disorders (such as inflammatory bowel disease, cardiovascular disease, breast cancer, etc.).^(30–32) The concentration of PAs in blood may vary significantly based on different sampling times after consumption of a BB diet. In our study, the highest dose of HA, 5 mg/kg/day, was given at 2 p.m.; by 9 a.m. the next day, its concentration in the serum was back to control levels (data not shown), indicating clearance of HA was less than 19 hours. Even with the short period of increase in HA level in the serum daily for just

2 weeks, we observed significantly increased bone formation. Moreover, considering the relatively low amount of HA given and its natural appearance in the blood after BB consumption, we believe that HA may have therapeutic values, although more detailed data are required.

Data from our current study suggest that activation of GPR109A occurs in osteoblasts or bone after treating osteoblastic cells or mice with HA. MAP kinase p38 activation and thereafter osteoblastic cell differentiation factor osterix transcription also appeared to be involved in the mechanisms of osteoblast differentiation by HA. Until now, the understanding of functional contribution of GPRs to bone development was limited to their role in maintaining mineral metabolism in the form of Ca²⁺ homeostasis stimulated by PTH or PTHrP.⁽³³⁾ Activation of GPR109A by HA leads to increased phosphorylation of p38, which can result in activation of osteoblast differentiation transcription factor osterix representing a novel signaling

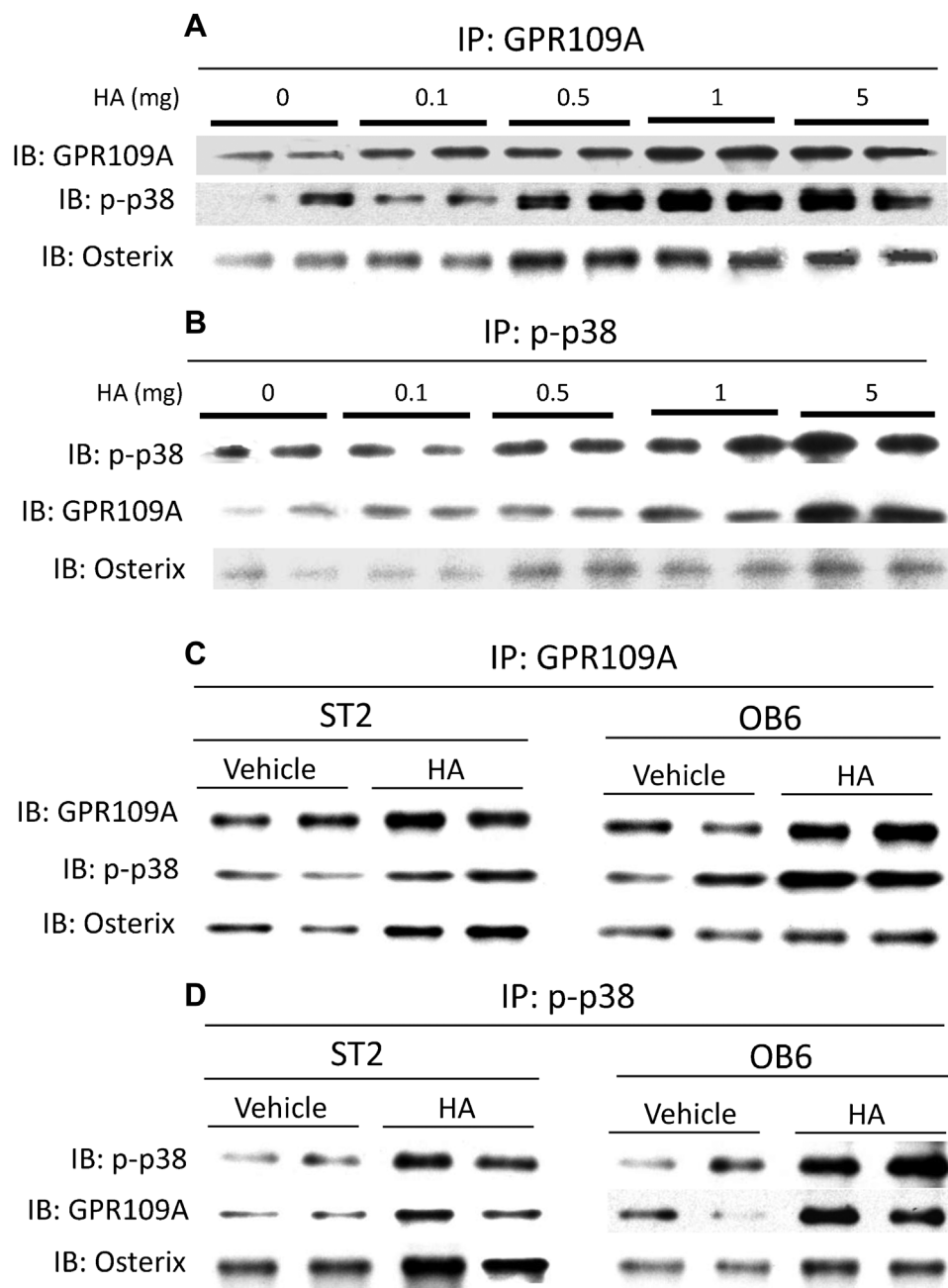


Fig. 5. HA increases association of GPR109A, p38, and osterix in bone and osteoblastic cells. Equal amount of bone protein of HA-treated mice (0 to 5 mg HA/kg BW) were immunoprecipitated (IP) using GPR109A or p-p38 antibodies and immunoblotted (IB) with GPR109A, p-p38 (phosphorylated p38), and osterix (A), or p-p38 antibodies and immunoblotted with p-p38, GPR109A, and osterix antibodies (B). (C) Immunoprecipitation with GPR109A antibodies in proteins isolated from ST2 or OB6 cells treated with either vehicle or HA 1× for 24 hours. (D) Immunoprecipitation with p-p38 antibodies in proteins isolated from ST2 or OB6 cells treated with either vehicle or HA 1× for 24 hours. Three mice were used for western blot in vivo samples, and for in vitro study, duplicated treatment was performed.

mechanism for which increased bone formation occurs in mice after HA treatment.

On the other hand, based on the data presented in the current study (Fig. 2), it will also be necessary to elucidate details of the negative effect of HA on bone marrow adipogenesis in our future studies. In the presence of HA, differentiation of adipocyte-like cells from mesenchymal stromal cells by rosiglitazone was significantly inhibited. Moreover, after treatment of HA for

12 days, committed pre-adipocyte 3T3-L1 cells exhibited an osteoblastic phenotype with increased ALP activity. It is not known whether HA directly suppresses transcription of adipogenesis, or whether it is a GPR109A-mediated action, or if activation of osteogenic signaling itself in turn suppresses bone marrow adipogenesis. It is also not known whether PAs would have similar inhibitory actions on adipogenesis in adipose tissue. However, knocking down of GPR109A gene in mesenchymal

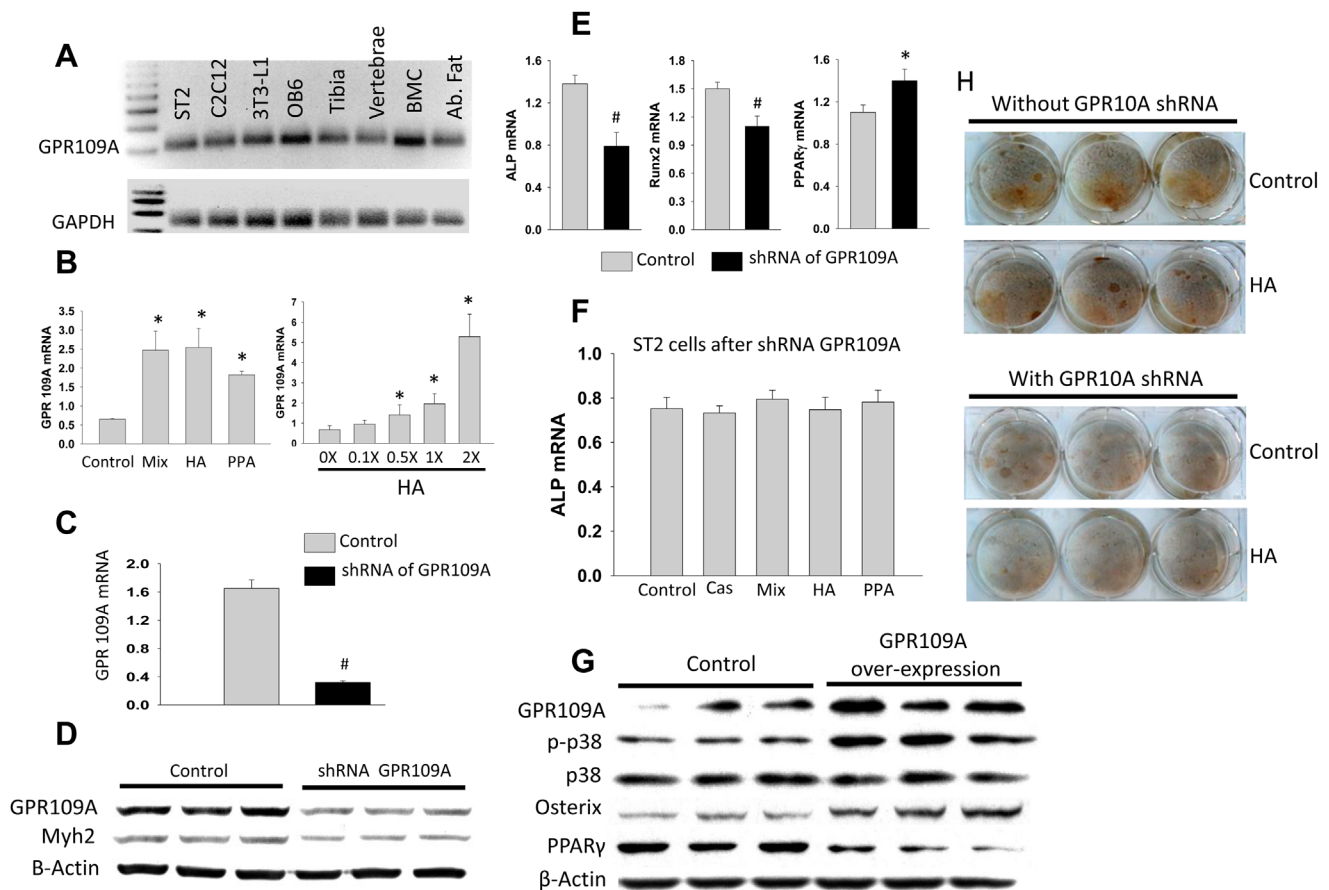


Fig. 6. GPR109A is required for PA to stimulate osteoblast differentiation. (A) GPR109A expression in various tissues and cells (BMC = bone marrow cells; Ab. Fat = abdominal fat). (B) PA stimulates GPR109A expression in ST2 cells. (C) GPR109A mRNA expression after GPR109A silencing in ST2 cells using shRNA. (D) GPR109A and myosin (Myh) protein expression after GPR109A silencing in ST2 cells using shRNA (triplicates). (E) Decreased ALP and Runx2 but increased PPAR γ mRNA expression in ST2 cells after shRNA GPR109A for 24 hours. (F) Treatment of PAs (24 hours) had no effects on stimulating ALP gene expression after shRNA of GPR109A in ST2 cells (control = vehicle treatment; cas = 2.5% serum from casein diet animals; Mix = a PA mixture similar to their concentration appeared in BB diet animal serum; HA 1 \times ; PPA, 3-(3-hydroxyphenyl)-propionic acid 1 \times). (G) Western blots showing overexpression of GPR109A in ST2 cells induces p38 and osterix activation but inhibits PPAR γ expression in triplicates. (H) von Kossa staining showing bone cell mineralization with or without GPR109A shRNA. ST2 cells were cultured for 25 days in the presence or absence of 1 \times HA with osteogenic media (with ascorbic acid and beta-glycerol phosphate). Data bars are expressed as mean \pm SEM from triplicates. Control and 0 \times , vehicle treated. Significant differences indicated by $p < 0.05$, * compared with either control or 0 \times treatment.

stromal ST2 cells resulted in decreased expression of endogenous PPAR γ gene, which is a well-known master gene for adipogenesis, indicating GPR109A may be involved in the course of adipogenesis.

Of the downstream targets of GPR109A-mediated signaling pathway for PA in bone cells, MAP kinase appears to be a key mediator. P38 MAPKs are activated in response to many extracellular stimuli, including growth factors, cytokines, and environmental stress.⁽³⁴⁾ The p38 MAPK pathway has been shown to be important for mineralization and development of osteoprogenitors and bone regeneration of mesenchymal stem cells.⁽¹⁴⁾ This may be because p38 MAPK can regulate canonical Wnt- β -catenin signaling by inactivation of GSK3 β .⁽³⁵⁾ We have shown that p38 MAPK was not only activated by BB but also that inhibition of p38 phosphorylation eliminated β -catenin nuclear translocation.⁽¹¹⁾ These results indicated that activation of p38 MAPK potentiates downstream Wnt signaling cascades and the

activation of Runx2 in bone and osteoblasts after BB feeding. In the current study, we present further evidence suggesting that p38 is involved in the transcription of osterix, which is known as an essential transcription factor for osteoblastogenesis. PAs activate this association of p38 and osterix in bone and osteoblasts after the activation of GPR109A. To further elucidate the involvement of GPR109A in osteogenesis, specific gene knockout animal models may be needed. We have published data suggesting that PA-activated membrane and cytosolic molecules may be reorganized by cytoskeletal motor proteins, such as myosin, to exert their functions. Data presented in the current study support the hypothesis that myosin may play a role in osteoblast differentiation⁽³⁶⁾ and that p38 may also be regulated by myosin.

In conclusion, we have identified PAs, metabolites derived from BB polyphenols that circulate in the blood after consumption of BB, as bioactive dietary factors capable of

acting on pluripotent stem cells found in bone of young rodents. Bone growth was increased in mice injected ip with HA, and this was associated with greater mRNA expression of ALP, GPR109A, and osterix, and increased osteoblastogenesis. Bone marrow-derived pre-adipocytes treated in vitro with HA took on phenotypical attributes similar to osteoblasts. PAs potentially inhibit adipogenesis in bone through reducing PPAR γ gene expression, and stable transfection studies suggest that GPR109A may regulate adipogenesis in bone by suppressing expression of PPAR γ . These findings may have profound implications for bone health, and more generally for the regulation of body composition and thus health issues such as obesity, insulin resistance, cardiovascular disease, gastrointestinal disorders, and others.

Disclosures

All authors state that they have no conflicts of interest.

Acknowledgments

We thank Matt Ferguson and Trae Pittman for their technical assistance. This study was supported by ARS CRIS #6251-51000-005-03S.

Authors' roles: J-RC designed the study and wrote the paper; OPL and JZ performed the experiment; MLB helped write the paper. MJJR and TMB helped design the animal study.

References

1. Bonjour JP, Chevalley T, Rizzoli R, Ferrari S. Gene-environment interactions in the skeletal response to nutrition and exercise during growth. *Med Sport Sci.* 2007;51:64–80.
2. Osteoporosis prevention, diagnosis, and therapy. NIH Consensus Statement. 2000 March 27–29;17:1–36.
3. Davies JH, Evans BA, Gregory JW. Bone mass acquisition in healthy children. *Arch Dis Child.* 2005;90:373–8.
4. Tyllavsky FA, Holliday K, Danish R, Womack C, Norwood J, Carbone L. Fruit and vegetable intakes are an independent predictor of bone size in early pubertal children. *Am J Clin Nutr.* 2004;79:311–7.
5. Lanham SA. Fruit and vegetables: the unexpected natural answer to the question of osteoporosis prevention? *Am J Clin Nutr.* 2006;83:1254–5.
6. Setchell KD, Lydeking-Olsen E. Dietary phytoestrogens and their effect on bone: evidence from in vitro and in vivo, human observational, and dietary intervention studies. *Am J Clin Nutr.* 2003;78(3 Suppl):593S–609S.
7. Rodan GA, Martin TJ. Therapeutic approaches to bone diseases. *Science.* 2000;289:1508–14.
8. Ogita M, Rached MT, Dworakowski E, Bilezikian JP, Kousteni S. Differentiation and proliferation of periosteal osteoblast progenitors are differentially regulated by estrogens and intermittent parathyroid hormone administration. *Endocrinology.* 2008;149:5713–23.
9. Engler AJ, Sen S, Sweeney HL, Discher DE. Matrix elasticity directs stem cell lineage specification. *Cell.* 2006;126:677–89.
10. Treiser MD, Yang EH, Gordonov S, Cohen DM, Androulakis IP, Kohn J, Chen CS, Moghe PV. Cytoskeleton-based forecasting of stem cell lineage fates. *Proc Natl Acad Sci USA.* 2010;107:610–5.
11. Chen JR, Lazarenko OP, Wu X, Kang J, Blackburn ML, Shankar K, Badger TM, Ronis MJ. Dietary-induced serum phenolic acids promote bone growth via p38 MAPK/ β -catenin canonical Wnt signaling. *J Bone Miner Res.* 2010;25:2399–411.
12. Ahmed K, Tunaru S, Offermanns S. GPR109A, GPR109B and GPR81, a family of hydroxy-carboxylic acid receptors. *Trends Pharmacol Sci.* 2009;30:557–62.

13. Latronico AC, Hochberg Z. G protein-coupled receptors in child development, growth and maturation. *Sci Signal.* 2010;3(143):re7.
14. Chang J, Sonoyama W, Wang Z, Jin Q, Zhang C, Krebsbach PH, Giannobile W, Shi S, Wang CY. Noncanonical Wnt-4 signaling enhances bone regeneration of mesenchymal stem cells in craniofacial defects through activation of p38 MAPK. *J Biol Chem.* 2007;282:30938–48.
15. Mårtensson UE, Salehi SA, Windahl S, Gomez MF, Swärd K, Daszkiewicz-Nilsson J, Wendt A, Andersson N, Hellstrand P, Grände PO, Owman C, Rosen CJ, Adamo ML, Lundquist I, Rorsman P, Nilsson BO, Ohlsson C, Olde B, Leeb-Lundberg LM. Deletion of the G protein-coupled receptor 30 impairs glucose tolerance, reduces bone growth, increases blood pressure, and eliminates estradiol-stimulated insulin release in female mice. *Endocrinology.* 2009;150:687–98.
16. Vinolo MA, Hirabara SM, Curi R. G-protein-coupled receptors as fat sensors. *Curr Opin Clin Nutr Metab Care.* 2012;15:112–6.
17. Sassa S, Kikuchi T, Shinoda H, Suzuki S, Kudo H, Sakamoto S. Preventive effect of ferulic acid on bone loss in ovariectomized rats. *In Vivo.* 2003;17:277–80.
18. Chen JR, Lazarenko OP, Blackburn ML, Badeaux JV, Badger TM, Ronis MJ. Infant formula promotes bone growth in neonatal piglets by enhancing osteoblastogenesis through bone morphogenic protein signaling. *J Nutr.* 2009;139:1839–47.
19. Bouxsein ML, Boyd SK, Christiansen BA, Guldberg RE, Jepsen KJ, Müller R. Guidelines for assessment of bone microstructure in rodents using micro-computed tomography. *J Bone Miner Res.* 2010;25:1468–86.
20. Cao JJ, Gregoire BR, Gao H. High-fat diet decreases cancellous bone mass but has no effect on cortical bone mass in the tibia in mice. *Bone.* 2009;44:1097–104.
21. Dempster DW, Compston JE, Drezner MK, Glorieux FH, Kanis JA, Malluche H, Meunier PJ, Ott SM, Recker RR, Parfitt AM. Standardized nomenclature, symbols, and units for bone histomorphometry: a 2012 update of the report of the ASBMR Histomorphometry Nomenclature Committee. *J Bone Miner Res.* 2013;28:2–17.
22. Chen JR, Singhal R, Lazarenko OP, Liu X, Hogue WR, Badger TM, Ronis MJ. Short term effects on bone quality associated with consumption of soy protein isolate and other dietary protein sources in rapidly growing female rats. *Exp Biol Med (Maywood).* 2008;233:1348–58.
23. Chen JR, Lazarenko OP, Shankar K, Blackburn ML, Badger TM, Ronis MJ. A role for ethanol-induced oxidative stress in controlling lineage commitment of mesenchymal stromal cells through inhibition of Wnt/ β -catenin signaling. *J Bone Miner Res.* 2010;25:1117–27.
24. Chen JR, Zhang J, Lazarenko OP, Kang P, Blackburn ML, Ronis MJ, Badger TM, Shankar K. Inhibition of fetal bone development through epigenetic down-regulation of HoxA10 in obese rats fed high-fat diet. *FASEB J.* 2012;26:1131–41.
25. Gregoire FM, Smas CM, Sul HS. Understanding adipocyte differentiation. *Physiol Rev.* 1998;78:783–09.
26. Tang W, Zeve D, Seo J, Jo AY, Graff JM. Thiazolidinediones regulate adipose lineage dynamics. *Cell Metab.* 2011;14:116–22.
27. Zhang J, Lazarenko OP, Blackburn ML, Shankar K, Badger TM, Ronis MJ, Chen JR. Feeding blueberry diets in early life prevent senescence of osteoblasts and bone loss in ovariectomized adult female rats. *PLoS One.* 2011;6(9):e24486.
28. Trzeciakiewicz A, Habauzit V, Horcajada MN. When nutrition interacts with osteoblast function: molecular mechanisms of polyphenols. *Nutr Res Rev.* 2009;22:68–81.
29. Ren N, Kaplan R, Hernandez M, Cheng K, Jin L, Taggart AK, Zhu AY, Gan X, Wright SD, Cai TQ. Phenolic acids suppress adipocyte lipolysis via activation of the nicotinic acid receptor GPR109A (HM74a/PUMA-G). *J Lipid Res.* 2009;50:908–14.
30. Biasi F, Astegiano M, Maina M, Leonarduzzi G, Poli G. Polyphenol supplementation as a complementary medicinal approach to treating inflammatory bowel disease. *Curr Med Chem.* 2011;18:4851–65.
31. Rodrigo R, Gil D, Miranda-Merchak A, Kalantidis G. Antihypertensive role of polyphenols. *Adv Clin Chem.* 2012;58:225–54.

32. Castillo-Pichardo L, Dharmawardhane SF. Grape polyphenols inhibit akt/mammalian target of rapamycin signaling and potentiate the effects of gefitinib in breast cancer. *Nutr Cancer*. 2012;64:1058–69.
33. Brown EM, Pollak M, Hebert SC. The extracellular calcium-sensing receptor: its role in health and disease. *Annu Rev Med*. 1998;49:15–29.
34. Martín-Blanco E. p38 MAPK signalling cascades: ancient roles and new functions. *Bioessays*. 2000;22:637–45.
35. Bikkavilli RK, Feigin ME, Malbon CC. p38 mitogen-activated protein kinase regulates canonical Wnt-beta-catenin signaling by inactivation of GSK3beta. *J Cell Sci*. 2008;121(Pt 21):3598–607.
36. Zimmerman SG, Thorpe LM, Medrano VR, Mallozzi CA, McCartney BM. Apical constriction and invagination downstream of the canonical Wnt signaling pathway require Rho1 and Myosin II. *Dev Biol*. 2010;340:54–66.